ACS Catalysis

Perspective

pubs.acs.org/acscatalysis

Catalysis Science of Bulk Mixed Oxides

Israel E. Wachs* and Kamalakanta Routray

Operando Molecular Spectroscopy and Catalysis Laboratory, Department of Chemical Engineering, Lehigh University, Bethlehem, Pennsylvania 18015, United States

ABSTRACT: Bulk mixed oxide catalysts are widely used for various applications (selective oxidation catalysts, electrocatalysts for solid oxide fuel cells, and solid oxide electrolyzers for the production of hydrogen), but fundamental understanding of their structure−performance relationships have lagged in the literature. The absence of suitable surface composition and surface structural characterization techniques and methods to determine the number of catalytic active sites, with the latter needed for determination of specific reaction rates (e.g., turnover frequency (1/s)), have hampered the development of sound fundamental concepts in this area of heterogeneous catalysis. This Perspective reviews the traditional concepts that have been employed to explain catalysis by bulk mixed oxides (molybdates, vanadates, spinels, perovskites, and several other specific mixed oxide systems) and introduces a modern perspective to the fundamental surface structure−activity/selectivity relationships for bulk mixed oxide catalysts. The new insights have recently been made available by advances in surface characterization techniques (low-energy ion scattering, energy-resolved XPS, and CH_3OH-IR) that allow for direct analysis of the outermost surface layer of bulk mixed metal oxide catalysts. The new findings sound a note of caution for the accepted hypotheses and concepts, and new catalysis models need to be developed that are based on the actual surface features of bulk mixed oxide catalysts.

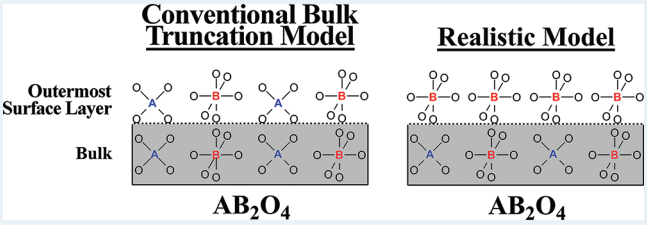

KEYWORDS: *catalysts, oxides, bulk, one component, mixed, vanadates, molybdates, spinels, perovskites, spectroscopy, in situ, Raman, IR, TPSR, LEIS, SIMS, XPS*

I. INTRODUCTION

Bulk mixed oxides are widely employed in industry as heterogeneous catalysts for selective oxidation reactions (e.g., methanol oxidation to formaldehyde, propylene oxidation/ammoxidation to acrolein/acrylonitrile, propane oxidation/ammoxidation to acrolein/acrylonitrile, *n*-butane oxidation to maleic anhydride, etc.), and electrocatalysts for solid oxide fuel cells and solid oxide electrolyzers for the production of hydrogen have received much attention in the catalysis literature over the past five decades.[1−4] The complexity of bulk mixed oxide catalyst powders (e.g., variable oxidation states, variable coordination for each oxidation state, chemical nature of surface sites (redox, basic, or acidic (Lewis or Bronsted)), participation of surface and bulk lattice oxygen atoms in oxidation reactions and presence of vacancies or defects) and difficulty in characterizing the surfaces of such low surface area catalytic materials (typically ∼1−10 m^2/g) have limited the development of the catalysis science of bulk mixed oxides. The difficulty in obtaining fundamental surface information about the topmost outer layer of low-surface-area bulk mixed oxides is a consequence of the inability of most characterization techniques (e.g., XPS, XANES/EXAFS, Raman, IR, EPR, NMR, XRD, HR-TEM, etc.) to discriminate between the same elements present both in the outermost surface layer and the bulk layers below the surface because the characterization measurements are dominated by the bulk signals.[5] The almost complete lack of surface information about the outermost surface layer of bulk mixed oxide catalysts has resulted in a catalysis paradigm in which the catalytic performance is correlated with bulk structural features routinely accessed by XRD or HR-TEM.[1] Furthermore, it was also typically assumed that the surfaces of bulk mixed oxides are just terminations of one of the bulk crystalline planes. Such a catalysis paradigm is problematic, since heterogeneous catalysis is a surface phenomenon, and the catalytic performance needs to be related to the surface characteristics (composition, morphology, coordination, oxidation state(s), and chemical properties).[6−8]

The paradigm of correlating the catalytic performance of bulk mixed oxides with their bulk crystalline structures has resulted in numerous explanations to account for the catalytic properties of bulk mixed oxides over the years. The first concept introduced into the catalysis literature stated that the catalytic activity of bulk mixed oxides was related to the short M═O bond present in the bulk structure, which implies that the short M═O bond is the catalytic active site.[9] This resulted in the appearance of many catalysis publications that attempted to correlate the M═O bond length or strength with catalytic activity and has become a cornerstone in the catalysis by bulk mixed oxides.[10−12]

A second concept introduced early into the catalysis literature of bulk mixed metal oxides was that the surfaces

Received: October 24, 2011
Revised: February 20, 2012
Published: April 30, 2012

   dx.doi.org/10.1021/cs2005482 | ACS Catal. 2012, 2, 1235−1246

were bifunctional, with one component responsible for dissociation of molecular O_2 and the second component responsible for chemisorption of hydrocarbons and redox (C−H bond breaking and oxygen insertion).[13,14] The selective oxidation of olefins by bismuth molybdate catalysts has been assumed to take place via a bifunctional mechanism in which the first site (BiOx) chemisorbs propylene to form a surface allyl ($H_2C{-}CH{-}CH_2$*) and the second site (MoOx) oxidizes the surface allyl intermediate.[13] The concept of contact synergy was introduced to explain the promotion of one phase by the addition of a second phase by invoking that a contact potential is created at the junction of two phases that favorably modifies the electronic density of the first catalytic active phase.[15−18]

An alternative explanation for the synergistic effect of two metal oxide phases in contact during selective oxidation reactions is the remote control theory.[19] According to the remote control theory, the catalyst is composed of two well-defined oxide phases: an acceptor and a donor phase. The acceptor phase is the center for hydrocarbon activation and can have, when alone, a low catalytic activity for the selective oxidation reaction. The donor phase generally has no selective oxidation activity, and its role is to produce activated oxygen at a high rate, which spills over to the acceptor phase and accelerates the catalytic reaction.

It was also postulated that isolation of the catalytic active sites from each other on the catalyst surface is required for selective oxidation reactions to occur.[20] According to this hypothesis, the reactive surface lattice oxygen atoms must be isolated from each other as an isolated grouping or a domain for the catalyst surface to be selective toward the desired product. For example, it was proposed that isolated surface lattice oxygen domains containing two to five adjacent reactive surface oxygen atoms selectively oxidize propylene to acrolein, whereas lattice oxygen domains containing more than five adjacent reactive surface oxygen atoms would lead to complete combustion of propylene.[20] This hypothesis was ascribed to assist in the discovery of $K_2O{-}V_2O_5$,[21] bismuth molybdates,[21] USb_3O_{10},[22,23] and $FeSb_xO_y$ selective oxidation catalyst systems.[24] The chronological development of the above concepts is given in Table 1 and reveals that these concepts

Table 1. Chronological Development of Concepts for Bulk Mixed Oxide Heterogeneous Catalysts

year	concept	references
1954	short M═O bond is catalytic active site	9−12
1963	site isolation	20−23
1973	bifunctional sites	13, 14
1979	contact synergy	15
1987	remote control	19

were developed in the 1954−1979 time frame, which precedes the development of modern catalysis science over the past three decades. Although these concepts have generally been accepted by the heterogeneous catalysis community researching bulk mixed oxides over time, there does not appear to be supporting data for these concepts, nor have the concepts ever been rigorously examined. Furthermore, none of the earlier studies provided any direct information about the nature of the surfaces of bulk mixed oxides, static as well as dynamic, under reaction conditions, and these early studies just tacitly assumed that the bulk mixed oxides just terminate with one of their bulk crystallographic planes.

In recent years, physical and chemical characterization methods have been developed that are capable of providing fundamental information about the characteristics of the outermost surface layer of bulk mixed metal oxide catalytic materials. Low-energy ion scattering (LEIS) quantitatively provides the elemental composition of the outermost surface layer (escape depth of ∼0.3 nm).[25] LEIS spectroscopy functions by analyzing the kinetic energy of scattered low-energy ions from the outer surface, since the kinetic energy is a function of the specific elemental masses present on the outermost surface. Although conventional X-ray photoelectron spectroscopy possesses an escape depth of ∼1−3 nm that is dominated by the signal from the layers below the outermost surface layer, the new energy-resolved XPS methodology (ER-XPS) method tunes the excitation energy to control the depth from which the measurement is performed and provides depth profile elemental composition information.[26,27] Depth profile elemental composition can also be obtained with coupled sputtering-LEIS studies that systematically peel off the outer layers. Recent advances in high resolution-transmission electron microscopy (HR-TEM) that allow for atomic resolution are making it possible to also examine the elemental composition of the surface region of some bulk mixed oxide catalysts and are revealing that amorphous surface oxide layers can also be present on such well crystallized bulk mixed oxides that effectively encapsulate the bulk mixed oxide crystals.[28−31]

In addition to the above physical characterization techniques, the outermost surface of bulk mixed metal oxides can also be chemically probed, since molecules cannot diffuse into the bulk of mixed oxides. Finding the proper molecule for metal oxides has been a challenge, since chemical methods employed for quantitatively determining the number of catalytic active sites on metal catalysts (e.g., chemisorption of CO, H_2, and O_2) have not been found to be feasible with metal oxides.[32−44] Methanol, as well as some other small alcohols, has been found to be a "smart" chemical probe molecule that can quantify the number of catalytic active sites, nature of the sites (redox, basic or acidic), oxidation states of the sites, and their chemical reactivity (kinetics and selectivity).[45−51] Methanol-IR spectroscopic chemisorption measurements can distinguish among surface methoxy ($M{-}OCH_3$) species coordinated to different surface cation sites and, thereby, provides direct information about the surface coordination sites and surface composition.[48,49,52] Methanol-temperature programmed surface reaction (TPSR) spectroscopy also quantifies the number of catalytic active sites as well as provides information about their chemical and electronic properties (selectivity (redox, basic, or acidic), kinetics, and oxidation states).[53−59]

This Perspective will examine our current understanding of bulk mixed oxide catalysts (molybdates, vanadates, spinels, perovskites, and several other specific mixed oxide systems) through the new insights recently made available by the advances in surface characterization techniques that allow for direct analysis of the outermost surface layer of bulk mixed oxide catalysts. Before discussing bulk mixed oxides, it is necessary to initially review some of the surface chemistry of one-component oxides.

II. SURFACE DENSITY OF CATALYTIC ACTIVE SITES (Ns) ON ONE-COMPONENT OXIDES

In contrast to metal catalysis,[60] the lack of knowledge of the catalytic active site density (Ns: number of surface catalytic active sites per unit surface area of the catalyst) for bulk oxides

dx.doi.org/10.1021/cs2005482 | ACS Catal. 2012, 2, 1235−1246

has prevented determination of quantitative TOF values for bulk one-component and mixed oxide catalysts and not allowed for direct comparison of intrinsic catalytic activities among different catalysts and catalysis laboratories. Consequently, Ns and TOF values are rarely reported in the literature for oxide heterogeneous catalysts. The few catalyst studies that have attempted to estimate Ns values for bulk oxides have employed (i) bulk crystallographic structural models that assume the crystal surface terminates with the same structure as the bulk,[61] (ii) oxygen chemisorption,[36,62,63] (iii) gravimetric chemisorption,[46−49,52−54,64] (iv) CH_3OH-IR chemisorption measurements,[48] and (v) CH_3OH-TPSR spectroscopy.[28,65] The crystallographic approach assumes that the surface terminates with one of the bulk crystal planes, which is now known to be an incorrect assumption, since the surface composition/structure and bulk composition/structure are generally dissimilar. The O_2 chemisorption approach, which is preceded by an H_2 reduction pretreatment, overestimates the number of surface sites because oxide reduction and oxidation typically cannot be limited to only the topmost surface layer of oxides. The gravimetric, CH_3OH-IR, and CH_3OH-TPSR studies, however, do quantitatively yield Ns values, since they determine the number of probe molecules adsorbed under standard conditions, and both methods give the same surface density values of catalytic active sites when cross-checked. In addition to methanol, other small molecules, such as formic acid, ethanol, and propanol, can also be employed to provide quantitative Ns values.[66−69]

The limited publications that determined Ns values allowed for quantification of the corresponding catalytic TOF values, which are critical to fundamentally understand the surface chemistry of bulk oxide catalysts. Application of thermogravimetric methanol chemisorption measurements to bulk MoO_3 crystals revealed that methanol selectively chemisorbs at the edge plane of crystalline MoO_3, which contains surface Mo−OH functionalities, not on the basal plane that is populated by the surface Mo═O functionality.[28,48,52,54,70,71] The same holds true for crystalline V_2O_5[70] that crystallizes with nonisotropic platelet morphology. Bulk $Fe_2(MoO_4)_3$, however, is isotropic and does not possess platelet morphology, resulting in methanol chemisorption on all exposed sites, and, consequently, gives rise to a much higher Ns values.[48,53,54,58,70] For one-component oxides (CaO, SrO, BaO, Y_2O_3, TiO_2, ZrO_2, HfO_2, CeO_2, Nb_2O_5, Ta_2O_5, Cr_2O_3, WO_3, Mn_2O_3, Fe_2O_3, Co_3O_4, Rh_2O_3, NiO, PtO, PdO, CuO, Ag_2O, Al_2O_3, Ga_2O_3, In_2O_3, SnO_2, P_2O_5, Sb_2O_3, Bi_2O_3 and TeO_2), the average Ns value was found to be ∼3−4 μmol/m^2.[70] This simple example demonstrates the importance of quantitatively determining Ns values for oxide catalysts.

III. TURNOVER FREQUENCY (TOF) FOR ONE-COMPONENT OXIDES

With quantitative Ns values now developed for one-component and mixed oxides, it has finally become possible to determine quantitative TOF values for oxide catalysts.

For one-component oxide catalysts, TGA-based methanol chemisorption was employed to determine Ns and TOF values for methanol oxidation to redox products.[70] An added advantage of using the methanol oxidation chemical probe reaction is that its reaction products also reflect the nature of the types of catalytic active sites present on the surface, since redox sites primarily yield HCHO with some methyl formate (CH_3OOCH) and dimethoxymethane (DMM-$(CH_3O)_2CH_2$), acid sites produce dimethyl ether (DMM-CH_3OCH_3), and basic sites form CO_x (CO and CO_2) reaction products.[45,70]

The TOF_{redox} values for the one-component oxides were found to vary over a rather wide range of reactivity from 10^4 to 10^{-3}/s (PtO ≫ Ag_2O > PdO > Co_3O_4 ∼ Mn_2O_3 ∼ Cr_2O_3 > CuO ∼ NiO > V_2O_5 ∼ ZnO ∼ BiO_2 ∼ SnO_2 ∼ Fe_2O_3 > HfO_2 > MoO_3 > ZrO_2 ∼ CaO > MgO ∼ Sb_2O_3 ∼ TeO_2 > BaO ∼ La_2O_3). The TOF_{acid} values for the one-component oxides were found to vary from 10^0 to 10^{-4}/s (Ga_2O_3 ∼ Al_2O_3 > Fe_2O_3 > P_2O_5 ∼ WO_3 ∼ V_2O_5 > Ta_2O_5 ∼ MoO_3 > Nb_2O_5 > TiO_2 > SiO_2), with all the oxides possessing surface Lewis acid sites and only P_2O_5, WO_3, V_2O_5, and MoO_3 expected to contain some surface Bronsted acid sites for the calcined catalysts (∼500 °C). The corresponding TOF_{basic} values for the one-component oxides were found to vary from 10^2 to 10^{-4}/s (Cr_2O_3 ∼ Co_3O_4 > Mn_2O_3 ∼ Bi_2O_3 ∼ ZnO > In_2O_3 ∼ NiO ≫ ZrO_2 ∼ MgO ∼ Y_2O_3 ∼ SrO > BaO ∼ SiO_2 > TiO_2). Although PtO and Rh_2O_3 also exhibited high TOF_{basic} values, they were not included in the above list of TOF_{basic}, since the formation of CO_x from these oxides is thought to be the result of further oxidation of the initial redox products. An interesting aspect of this compilation of methanol oxidation TOF values for one-component oxides catalysts is that many of the oxides surfaces are multifunctional surfaces and not only exclusively consisting of redox, acidic, or basic sites.

The availability of the above quantitative methanol oxidation TOF_{redox} values allows for examination of correlations between the reactivity of the one-component oxide catalysts with several oxide properties.[71] A semilog plot of the TOF_{redox} vs the bulk heat of formation of the one-component oxides, which reflects the M−O bond strengths, does not show any apparent relationship between the TOF_{redox} and M−O bond strength of the oxide catalysts. It has also been claimed that isotopic $^{18}O_2$−$^{16}O_2$ exchange rates for oxides are related to the ease of oxygen removal from the metal oxide and its M−O bond strength.[72] However, a log−log plot of TOF_{redox} vs isotopic oxygen exchange rate constant does not show a correlation between these rates. A correlation was also not found for the log−log plot between the TOF_{redox} vs onset reduction temperature of the oxides from H_2-TPR measurements. The absence of a correlation between TOF_{redox} and onset of hydrogen reduction temperature is not surprising, given that there are several possible competing rate-determining steps in the reduction process (H−H bond breaking, O−H bond formation, or M−OH and MO−H bond breaking). Thus, it appears that the ease of oxygen removal from the one-component oxides is not related to the specific reaction rate for methanol oxidation to redox products.

A clear inverse correlation, however, does exist for the semilog plot of TOF_{redox} vs the surface methoxy (CH_3O*) decomposition temperature (Tp), presented in Figure 1, during CH_3OH-TPSR spectroscopy for catalysts exhibiting redox selectivity of 85−100% (with a regression error of <2%).[70] Given that the rate-determining step for methanol oxidation is breaking of the C−H bond of the surface methoxy intermediate,[73] such a strong correlation is not unexpected. Furthermore, a similar correlation is also found between TOF_{acid} and the surface methoxy decomposition temperature determined by CH_3OH-TPSR spectroscopy (with a regression error of <5%). For acid catalysis resulting in the formation of CH_3OCH_3, the reaction mechanism proceeds via the rate-determining step of C−O bond breaking of the surface methoxy intermediate.[74] These inverse correlations between

dx.doi.org/10.1021/cs2005482 | ACS Catal. 2012, 2, 1235−1246

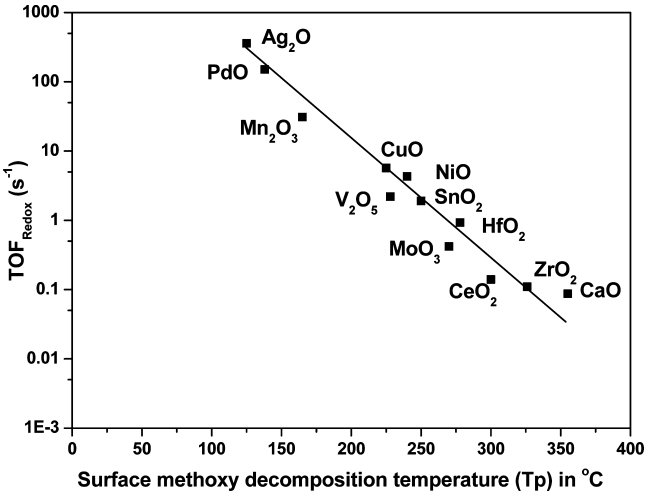

Figure 1. Semilog plot of TOF_{redox} vs surface methoxy decomposition temperature for one-component oxides (regression error < 2%).

TOF values and surface methoxy decomposition Tp reveal that the TOF values are directly related to the thermal stability of the surface methoxide intermediate: a less stable surface methoxy is more reactive, and a more stable surface methoxy is less reactive. Note that neither of these rate-determining steps depend on the catalyst M−O or M═O bond strengths or lengths that are thought to be related to the ease of oxygen removal from the metal oxides. That is why quantitative TOF values and metal oxide properties, especially bulk properties, do not correlate, since the reactivity of surface methoxy intermediates is primarily related to the surface methoxy C−H or C−O bond-breaking steps during the rate-determining steps.

According to literature models, the selectivity in Mars−van Krevelen oxidation reaction should be associated with oxygen mobility or the intrinsic activity of individual oxygen species (ease of oxygen removal).[75,76] This hypothesis implies that high oxygen mobility should result in overoxidation and low selectivity. A semilog plot of selectivity to redox products during methanol oxidation over oxides vs the rate of isotopic $^{16}O_2-^{18}O_2$ exchange, however, gives rise to a noncorrelated, random ("shot gun") plot.[70] A similar noncorrelated, random plot is obtained for the semilog plot of selectivity to redox products during methanol oxidation over oxides vs the TOF_{redox} values. Furthermore, the selectivity to redox products was 100% for many catalysts over a very wide range of TOF_{redox} values from 10^{-3} to 10^{3}/s (Ag_2O > PdO > CuO > SnO_2 > HfO_2 > CeO_2 > TeO_2 > Sb_2O_3 > La_2O_3). The absence of any apparent correlations between oxygen mobility or ease of oxygen removal for metal oxides and the reaction rates for oxidative dehydrogenation of methanol suggests that the redox selectivity is primarily associated with the chemical properties of the specific oxide catalytic active sites.

IV. NATURE OF CATALYTIC ACTIVE SITES FOR BULK MIXED OXIDE CATALYSTS

In heterogeneous catalysts, the properties of the outermost surface layer are of paramount importance, since the catalytic active sites and reaction intermediates reside only at the outermost surface layer of heterogeneous catalysts. Researchers in the field of bulk mixed metal oxide catalysis, however, have almost exclusively focused on the bulk crystallographic structures and thermodynamics, as depicted in the above correlations, and almost no relevant surface information about bulk mixed oxide catalysts exist. The few attempts to characterize the surfaces of bulk mixed oxide catalysts primarily employed XPS, which dilutes the signal from the outermost surface layers with the signals from multiple layers below the surface (∼1−3 nm). Consequently, XPS is not able to satisfactorily provide chemical information about the outermost surface layer of bulk mixed oxide catalysts.[27] As already mentioned, in the absence of meaningful surface information about bulk mixed oxide catalysts, it was tacitly assumed that the surface is just an extension of the bulk mixed oxide structure, and an exposed crystallographic plane was arbitrarily selected.[77−83] Surface characterization methods developed in recent years, however, directly demonstrate that for many mixed oxide systems, the surface composition of bulk mixed oxide catalysts is remarkably different from that present in the bulk structure.

a. Bulk Mixed Molybdates and Vanadates. Recent LEIS measurements revealed that the outermost surface layer of bulk mixed molybdates and vanadates tend to be enriched with amorphous surface MoO_x and VO_x species.[27] These amorphous overlayers are also apparent in HR-TEM images, and elemental compositional analysis of the overlayers confirms that they are enriched in redox V and Mo components.[28,29] In some cases, the surface enrichments even approach monolayer coverage that cannot be simply accounted by preferential termination of bulk crystalline planes.[27] This is also consistent with in situ CH_3OH-IR chemisorption experiments that reveal only the presence of surface Mo−OCH_3 and V−OCH_3 species on the bulk mixed molybdate and vanadate catalysts.[28,29,48,49] Furthermore, CH_3OH-TPSR exhibits the surface chemistry of only Mo-OCH_3 and V-OCH_3 rather than that of the non-Mo or -V, respectively, metal oxide components.

Surface enrichment with MoO_x and VO_x for bulk mixed molybdates and vanadates, respectively, appears to be limited to the first few outer layers of the bulk mixed metal oxides. HR-TEM images of bulk mixed molybdate and vanadate catalysts reveal an amorphous layer, ∼1 nm, that is enriched with Mo and V, respectively.[28,32] Depth profile compositional information with sputtering LEIS spectroscopy and the very new method of energy-resolved XPS (ER-XPS) reveals that the surface enrichment is limited to only the outermost surface layer or the two topmost layers.[26,27]

b. Bulk Mixed Oxide Spinels. Bulk mixed oxide *normal* spinels possess the general formula

$$A^{2+(Td)}B_2{}^{3+(Oh)}O_4 \quad (1)$$

In the bulk normal spinels, the A cation has AO_4 coordination and the B cations contain BO_6 coordination. The compositions of the outermost surface layer for several bulk mixed oxide normal spinels were determined with LEIS, and for all systems, the surface concentrations of the A^{2+} were markedly diminished relative to the bulk B/A = 2 ratio. For $CoAl_2O_4$ and $ZnAl_2O_4$, it was surprisingly found that only traces of the Co^{2+} and Zn^{2+} cations are present on the spinel surface that almost exclusively consists of Al^{3+} cations and O^{2-} anions.[84−87] For the $ZnCo_2O_4$ normal spinel that consists of tetrahedral-coordinated Zn^{2+} and octahedral-coordinated Co^{3+} sites, however, it was found that the surface almost exclusively consists of Co sites.[88] These findings suggest that the tetrahedral A cations possess low stability on the mixed oxide spinel surfaces and, consequently,

dx.doi.org/10.1021/cs2005482 | ACS Catal. 2012, 2, 1235−1246

prefer the tetrahedral sites below the surface, which leaves the octahedral B cations the dominant surface cations. For a series of Mn-containing spinels, however, it was found that because of an oxidative transfer, much more Mn was on the surface.[85] In contrast, the much larger sampling depth of XPS measures both the octahedral and tetrahedral cations in the mixed oxide spinels. Most importantly, only the compositions of the outermost surface layer determined with LEIS were found to track the catalytic activity of mixed oxide spinels.[85,89−93]

Bulk mixed oxide *inverse* spinels possess the general formula

$$B^{3+(Td)}A^{2+(Oh)}B^{3+(Oh)}O_4 \quad (2)$$

Bulk inverse spinels have the same structure as bulk normal spinels, but their cations are inversed (one of the two B^{3+} cation has BO_4 coordination and the A^{2+} cation contains AO_6 coordination). Consequently, the A cation is now present in octahedral sites in inverse spinels and, thus, should also be present on the outermost surface layer, whereas the concentration of the B cation should now decrease because one of the B cations is located at tetrahedral sites. Indeed, this is what was found for the $MgFe_2O_4$ inverse spinel, $Fe^{3+(Td)}Mg^{2+(Oh)}Fe^{3+(Oh)}$, which gives a strong Mg LEIS signal, in contrast to tetrahedral Zn^{2+} in the $ZnFe_2O_4$ normal spinel, and the Fe LEIS signal is half that for the $ZnFe_2O_4$ normal spinel.[94]

Thus, the surface compositions of normal and inverse spinels do not correspond to their bulk stoichiometry and depend on the local coordination of the A and B sites, since only octahedral sites are present on the outermost surface layer of bulk mixed oxide spinels.

c. Bulk Mixed Oxide Perovskites. Normal perovskites have the general formula

$$A^{2+(tw)}B^{4+(Oh)}O_3 \quad (3)$$

In normal perovskites, the A cation contains AO_{12} coordination, and the B cation possesses BO_6 coordination. LEIS analysis of the outermost surface layer of dense sintered $SmCoO_3$ perovskite revealed that Sm is the dominant surface cation, with the Co cation present at only 5% of its bulk composition.[95] Preferential surface segregation of Ba for the $BaZrO_3$ perovskite was also found, but the surface Ba enrichment was not as pronounced as for Sm for $SmCoO_3$.[96] For the doubly substituted perovskite $(La_{0.6}Sr_{0.4})(Co_{0.2}Fe_{0.8})O_3$ composed of two different A cations and B cations, LEIS analysis reveals that the outermost surface layer primarily consists of Sr with some La and with no Co and Fe present.[97] Thus, bulk mixed oxide perovskites appear to terminate with preferential exposure of the (100)-AO planes that exclusively possess the A cations.

d. Bulk $Ce_xZr_{1-x}O_2$ Mixed Oxides. Bulk $Ce_xZr_{1-x}O_2$ mixed oxides are employed as oxygen storage catalysts in three-way automotive catalysts.[98] The oxygen mobility and thermal stability are enhanced when Zr is introduced into the CeO_2 lattice to form bulk $Ce_xZr_{1-x}O_2$ mixed oxides.[99−105] The surface chemical composition and oxidation states of the surface Zr and Ce cations were chemically probed with CH_3OH-IR spectroscopy.[106] Methanol chemisorbs as surface CH_3O* species, and the IR bands of the surface methoxy C−H and C−O vibrations for Zr−OCH_3 and Ce−OCH_3 reflect the cation surface composition and oxidation states, since the surface methoxy vibrations are dependent on the specific coordinated cation. The CH_3OH-IR spectroscopic measurements of oxidized surfaces indicate that there is no surface segregation of either Zr or Ce for the bulk $Ce_xZr_{1-x}O_2$ mixed oxides over the entire compositional range ($0 < x < 1$). Upon reduction, the CH_3OH-IR spectra demonstrate that surface Zr^{4+} does not reduce, and both surface Ce^{4+} and Ce^{3+} coexist, with the ratio of Ce^{3+}/Ce^{4+} increasing with extent of reduction. Consequently, it was possible to also monitor reoxidation of the surface Ce cations with different thermal treatments in different environments. Thus, CH_3OH-IR spectroscopy can be an excellent chemical probe that can determine the surface composition and oxidation states for many bulk mixed oxide catalyst systems.[48,52]

e. Summary. The newer methods of surface analysis of the outermost surface layer are showing that the surfaces of bulk mixed oxide catalysts may be very different from the bulk mixed oxide phases and are generally present as reconstructed surfaces. The driving force for surface enrichment and reconstruction is lowering of the oxide surface energy with the element and structure possessing the lowest surface energy becoming the dominant component and structure at the outermost surface layer. For example, (i) bulk $(VO)_2P_2O_7$ was determined with LEIS to have a surface P/V ratio of ∼2, whereas the bulk P/V stoichiometry is 1,[107] and LEIS analysis of the complex bulk Mo−V−Nb−Te−O catalyst reveals that the surface is enriched with V and Te, but depleted in Mo.[108] In addition, several in situ IR and Raman studies have revealed that even one-component metal oxides terminate with surface structures that are more similar to supported surface metal oxide species and not present in their bulk structures (e.g., V_2O_5,[109] Nb_2O_5,[110] Cr_2O_3,[111] WO_3[74]). Thus, the surface structures of even one-component oxide systems restructure relative to their bulk structures. Consequently, it is critical to obtain more insights into the surface compositions and structures of one-component and bulk mixed oxide catalysts for this field of heterogeneous catalysis to advance.

V. RELATIONSHIP BETWEEN M═O BOND LENGTH AND CATALYTIC ACTIVITY

To quantitatively examine the hypothesis of the relationship between the short M═O bond length in bulk mixed metal oxides and their catalytic reactivity, the surface reactivity of bulk mixed molybdate and vanadate catalysts was investigated using CH_3OH-temperature-programmed surface reaction (TPSR) spectroscopy and steady-state CH_3OH oxidation. The CH_3OH-TPSR experiment provides the first-order surface kinetic rate constants for breaking of the C−H bond of surface CH_3O* intermediates for the formation of HCHO and the number of catalytic active sites (Ns).[112] The corresponding steady-state methanol studies provide the specific reaction rate (TOF-number of methanol molecules converted to redox products per exposed surface active site per second) and the equilibrium adsorption constant (K_{ads}) that reflects breaking of the methanol O−H bond upon adsorption.[113] The number of exposed surface sites present for the bulk mixed oxides was quantitatively determined with CH_3OH chemisorption-IR spectroscopy measurements. Raman spectroscopy gives rise to sharp M═O bands that reflect the short M═O bond length.[114,115] The present study rigorously compares, for the first time, the relationship between the normalized surface reactivity for CH_3OH oxidation to formaldehyde and the short M═O bond lengths of bulk mixed molybdates and vanadates.

The bond lengths of short M═O bonds in the bulk lattice of mixed vanadates and molybdates were obtained from crystallo-

dx.doi.org/10.1021/cs2005482 | ACS Catal. 2012, 2, 1235−1246

graphic literature studies.[65] These bulk mixed oxides also possess a sharp M=O band in Raman spectroscopy. The Raman shift of the bulk vanadates and molybdates were also used to calculate the short M=O vibration.[114,115] The CH_3OH-TPSR surface kinetic parameters for the rate-determining step, k_{rds}, for HCHO formation over the bulk mixed vanadates and molybdates are plotted against the short M=O bond length in Figure 2a and b, respectively. No

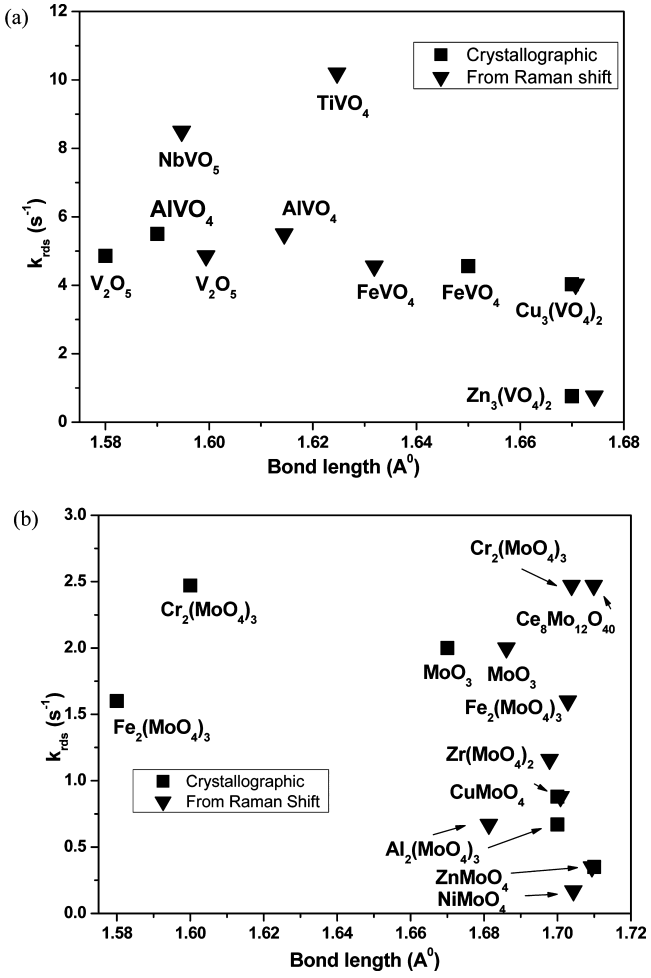

Figure 2. Plots of first-order rate constant (k_{rds}) for surface methoxy decomposition vs M=O bond lengths for (a) bulk mixed vanadates and (b) bulk mixed molybdates. The M=O bond lengths for the bulk vanadates and molybdates were determined from their crystallographic studies and shifts of the Raman bands. The metal−oxygen bonds with less than 1.7 Å and Raman shift greater than 900 cm^{-1} were taken as having a double-bond character for the purpose of this plot.

particular correlation can be seen between the short M=O bond lengths in the bulk lattice of mixed vanadates and molybdates and the surface catalytic activity, indicating that the length of the short M=O bond is not a controlling factor in catalytic oxidation reactions by bulk mixed oxides.

VI. RELATIONSHIP BETWEEN BULK HEAT OF FORMATION OF OXIDES AND CATALYTIC ACTIVITY

It was proposed in the 1960s that the larger the bulk heat of formation of oxides, the less active the catalysts.[116,117] Morooka et al. observed that reaction rates of oxides (such as Ag_2O, CuO, CO_3O_4, NiO, MnO_2, CdO, Fe_2O_3, V_2O_5, Cr_2O_3, CeO_2, ThO_2) for propylene, isobutene, acetylene, and ethylene oxidation are inversely related to their bulk heat of oxide formation.[116,117] It was reasoned that the bulk heat of formation of metal oxides is equivalent to the heat of formation of one bond, averaged over all the metal−oxygen bonds present. Therefore, the heat of formation is a representation of the metal−oxygen bond strength in the bulk mixed oxide. Similarly, Sachtler and de Boer correlated the qualitative activity, which was not normalized per surface area or number of exposed active sites, of bulk oxide catalysts with their reducibility.[118] The degree of reducibility is considered as the ease with which an oxygen atom could be removed from an oxygen−metal bond. Therefore, high reducibility corresponds to low activation energy for reduction and to low metal−oxygen bond energy. Thus, the ease of removal of oxygen from an oxide lattice leads to higher conversion and lower selectivity.

Briand et al., however, did not find a correlation between quantitative redox and basic TOF values for methanol oxidation to formaldehyde with the strength of the metal−oxygen bond of the bulk mixed oxides. These more recent results demonstrate that the rate-determining step of methanol oxidation over metal oxides does not involve the breaking of a surface metal−oxygen bond.[47] Similarly, Badlani et al. did not find a correlation between the quantitative TOF_{redox} and bulk heat of oxide formation for one-component oxides for methanol oxidation, as shown below in Figure 3.[70] Although

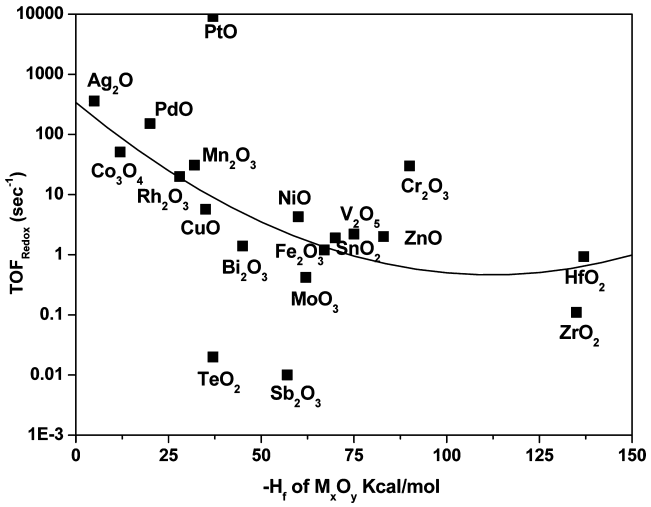

Figure 3. Semilog plot of TOF_{Redox} vs heat of formation of one-component oxide catalysts (regression error of 0.28).

qualitatively it appears that the TOF_{redox} decreases as the bulk heat of metal oxide formation increases, the curve in Figure 3 has a significant associated regression error of 0.28 with respect to the data points. A closer examination shows that (1) for the same approximate heat of formation of ∼35 kcal/mol, the TOF_{redox} varies by approximately a factor of 10^6, and (2) for the same TOF_{redox} value of ∼1/s, the bulk heat of oxide formation varies from ∼40 to 140 kcal/mol. These conclusions, based on rigorous quantitative data, are not surprising, given that the rate-determining step (rds) for methanol oxidation involves breaking of the C−H bond, not M−O bonds, of the catalyst.

dx.doi.org/10.1021/cs2005482 | ACS Catal. 2012, 2, 1235−1246

VII. CONTACT SYNERGY

The bulk iron molybdate catalyst is widely used in industry for the selective oxidation of methanol to formaldehyde. It has been reported in the catalysis literature that the presence of excess crystalline MoO_3 in the bulk $Fe_2(MoO_4)_3$ catalyst enhances the resulting catalytic performance during the selective methanol oxidation reaction.[119] Okamoto et al. proposed that the presence of excess MoO_3 in bulk iron molybdate catalysts is essential to produce stoichiometric $Fe_2(MoO_4)_3$ at the catalyst surface, which was thought to be the active phase for the selective oxidation of methanol to formaldehyde.[120] Soares et al. proposed that the active phase of the bulk iron molybdate catalyst has a Mo/Fe = 1.5 ratio of $Fe_2(MoO_4)_3$ and excess MoO_3 is required to replenish the loss of molybdenum oxide from the hot spot region of the reactor.[119] The increase in catalytic performance of bulk iron molybdate catalysts containing excess MoO_3 has also been attributed to the contact synergy between the excess MoO_3 and $Fe_2(MoO_4)_3$ phases.[121,122] The contact synergy explanation has also been put forth to explain the enhanced catalytic activity of other bulk metal molybdate ($NiMoO_4$, $CoMoO_4$, and $MnMoO_4$) phases in contact with excess crystalline MoO_3.[16−18] Recall that the contact synergy theory proposes that promotion of one phase occurs at the junction of the two metal oxide phases by creation of a contact potential that favorably modifies the electronic density of the catalytic active phase.

To examine if the contact synergy concept for the MoO_3/$Fe_2(MoO_4)_3$ applies to the iron molybdate catalyst system for the oxidation of methanol to formaldehyde, a model supported MoO_3/Fe_2O_3 catalyst was synthesized and examined for methanol oxidation.[28] The model supported MoO_3/Fe_2O_3 catalyst consists of a two-dimensional surface MoO_x monolayer on the Fe_2O_3 support and does not possess any molybdate crystalline phases, MoO_3 or $Fe_2(MoO_4)_3$, as demonstrated by in situ Raman and IR spectroscopy characterization. This amorphous surface MoO_x monolayer phase, however, was found to exhibit the same catalytic performance as bulk MoO_3/$Fe_2(MoO_4)_3$ catalysts without the presence of crystalline molybdate phases. The performance by the supported MoO_3/Fe_2O_3 catalyst during methanol oxidation demonstrates that only a surface MoO_x phase in contact with an FeO_x substrate, which forms a bridging Mo−O−Fe bond, is required to have a good performing iron molybdate catalyst and that contact between the crystalline MoO_3 and $Fe_2(MoO_4)_3$ phases is not a prerequisite for good catalytic performance. Furthermore, increasing the ratio of crystalline MoO_3 to $Fe_2(MoO_4)_3$ phases in the bulk iron molybdate catalyst does not affect the TOF (number of methanol molecules converted to HCHO per surface active site per second), but it does increase the formaldehyde selectivity by decreasing dimethyl ether (DME: CH_3OCH_3) production. The formation of DME takes place on the exposed FeO_x acidic sites, and the role of excess MoO_3 is simply to be a molybdenum oxide reservoir that supplies surface MoO_x species to cover the exposed FeO_x sites.

The above conclusion is further confirmed by the elemental composition of the outermost surface layer of the bulk MoO_3/$Fe_2(MoO_4)_3$ mixed oxide catalysts.[28] LEIS spectroscopy, with an escape depth of ∼0.3 nm, revealed that the MoO_3-free, stoichiometric bulk $Fe_2(MoO_4)_3$ phase is almost completely covered with surface MoO_x and that no exposed FeO_x sites are present in the absence of excess crystalline MoO_3. Corresponding in situ CH_3OH-IR spectroscopy measurements exhibit the presence of only surface Mo−OCH_3 intermediates, which is consistent with the surface of the bulk iron molybdate catalysts consisting of a surface MoO_x monolayer. The corresponding CH_3OH-TPSR spectroscopy study yields only formaldehyde and does form DME that is characteristic of exposed FeO_x acidic sites. HR-TEM images of the $MoO_3/Fe_2(MoO_4)_3$ mixed oxide catalysts indicate the presence of an amorphous layer of ∼1−2 nm present on the $Fe_2(MoO_4)_3$ phase in addition to the presence of MoO_3 crystallites.

The above fundamental studies with the model supported MoO_3/Fe_2O_3 monolayer and bulk $MoO_3/Fe_2(MoO_4)_3$ catalysts reveal that the contact synergy phenomenon is actually related to the presence of an amorphous molybdenum oxide layer between the two oxide phases, and the excess MoO_3 phase serves to maintain the surface MoO_x layer. The presence of enriched surface MoO_x and VO_x layers in many bulk mixed molybdate and vanadate catalysts has also been confirmed with LEIS spectroscopy[26] and CH_3OH chemical probe studies.[29,46−48] Thus, the presence of surface MoO_x and VO_x catalytic layers on the surfaces of bulk mixed oxides appears to be a general phenomenon that was completely not considered in formulating the contact synergy hypothesis.

VIII. REMOTE CONTROL

A related theory that has also been proposed in the catalysis literature to account for the synergistic effect of two metal oxide phases in contact during selective oxidation reactions is the remote control theory.[19] According to the remote control theory, the catalyst system is composed of two well-defined metal oxide phases, an acceptor phase and a donor phase. The acceptor phase is the center for hydrocarbon activation and can have, when alone, a low catalytic activity for the selective oxidation reaction. The donor phase generally has no selective oxidation activity, and its role is to produce activated oxygen at a high rate, which spills over to the acceptor phase, which accelerates the catalytic cycle. The remote control theory has been applied for the bulk Sb_2O_4−MoO_3 catalyst system, for which it was proposed that Sb_2O_4 is the donor phase and MoO_3 is the acceptor phase,[123] and the bulk SnO_2−MoO_3 catalyst system, for which it was claimed that SnO_2 is the donor phase and MoO_3 is the acceptor phase.[124]

The bulk Sb_2O_4−MoO_3 catalyst system was carefully examined with the aid of $^{18}O_2$ for oxygen spillover from Sb_2O_4 to MoO_3. No evidence, however, was detected with Raman spectroscopy for oxygen spillover from SnO_2 to MoO_3.[125] The Sb_2O_4−MoO_3 catalyst system was also carefully investigated with in situ Raman spectroscopy, and it was found that the bulk MoO_3 crystallites transform to surface MoO_x species on the SnO_2 support during thermal treatments.[126] Thermal dispersion of one metal oxide over another is well documented in the catalysis literature, and the driving force is to decrease the overall system surface free energy of the combined oxides.[127−129]

A prerequisite for spontaneous thermal dispersion is that the treatment temperature exceed the Tammann temperature, the temperature at which surface atoms begin to diffuse for the more mobile oxide. Given the relatively low Tammann temperature of ∼260 °C for bulk MoO_3, it is very easy to thermally spread MoO_3 over many static oxide supports that have much higher Tammann temperatures (e.g., SnO_2 ∼ 680 °C), which can act as oxide supports for the spreading of MoO_x species. The dispersion of bulk metal oxides with low

dx.doi.org/10.1021/cs2005482 | ACS Catal. 2012, 2, 1235−1246

Table 2. Surface Active Sites and Reactivity of One-Component Oxides toward Methanol Selective Oxidation at Low Conversion

				selectivity (%)					
oxide (reaction temp in °C)	S_{BET} (m^2/g)	N_s (μmol/m^2)	TOF[a] (s^{-1})	HCHO	CO_2	CO	DME	DMM	MF
CeO_2 (380)	2.4	4.8	1.3	100					
MnO (300)	0.8	1.6	31.0	79.5	20.5				
Cr_2O_3 (290)	3.0	12.4	7.1	35.7	59.6	4.7			
Al_2O_3[b] (300)	180.0	5.6	0.0				100.0		
NiO (300)	1.1	4.4	6.4	82.6	17.4				
CoO (270)	0.4	2.2	24.7	61.2	34.2				4.7
CuO (330)	0.3	7.0	15.9	100.0					
Fe_2O_3 (300)	21.4	3.2	3.3	57.9			36.4	1.2	4.5
ZnO (380)	5.3	0.3	18.2	32.7	31.5	22.9			12.8
Bi_2O_3 (450)	0.2	2.0	24.7	100.0					
MoO_3 (380)	5.0	0.7	5.3	84.1			15.9		

[a]Turnover frequency based on methanol partial oxidation products (formaldehyde, methyl formate and dimethoxymethane). [b]Ns, reaction rate (for TOF calculation), and selectivity values from refs 69, 130.

Table 3. Surface Active Sites and Reactivity of Bulk Mixed Molybdates and MoO_3 Catalysts toward Methanol Selective Oxidation

					selectivity (%)[c]		
catalyst	S_{BET} (m^2/g)	N_s (μmol/m^2)	reaction rate[a] (μmol/m^2 s)	TOF[b] (s^{-1})	HCHO	DME	DMM
$Ce_8Mo_{12}O_{49}$	4.0	12.0	46.5	3.3	86.5	13.5	
$MnMoO_4$	1.9	3.1	20.6	6.6	99.8		
$Cr_2(MoO_4)_3$	1.7	12.6	43.1	3.1	91.0	9.0	
$Al_2(MoO_4)_3$	2.8	5.0	9.4	1.8	26.1	73.9	
$NiMoO_4$	9.5	2.8	2.6	0.9	100.0		
$CoMoO_4$	5.5	4.1	4.4	0.9	88.2	11.8	
$CuMoO_4$	0.8	23.9	24.7	1.1	100.0		
$Fe_2(MoO_4)_3$	9.6	4.2	9.6	1.4	61.0	39.0	
$ZnMoO_4$	2.1	15.7	18.2	1.0	87.4	12.6	
$Bi_2Mo_3O_{12}$	0.2	16.5	23.4	1.4	100.0		
MoO_3	5.0	0.7	4.4	5.3	84.1	15.9	

[a]Activity based on overall methanol conversion at 380 °C. [b]Turnover frequency based on methanol partial oxidation products (formaldehyde and dimethoxymethane); reaction temperature = 380 °C. [c]Selectivity toward formaldehyde (FA), dimethyl ether (DME), and dimethoxymethane (DMM) at 380 °C.

Tammann temperatures over oxide supports can be further accelerated in the presence of certain reactive environments.[126] The enhanced catalytic activity of the thermally treated physical mixtures is related to the increase in the number of exposed catalytic sites (e.g., MoO_3 crystallites with a low number of exposed sites being transformed to surface MoO_x species that are highly dispersed) and the greater TOF of the surface MoO_x species compared with the active sites of crystalline MoO_3. Thus, it is not oxygen that is being transported from the SnO_2/Sb_2O_4 donor phases to the MoO_3 acceptor phase, but it is mobile MoO_x that is being transported from the MoO_3 crystallites to the surfaces of the SnO_2/Sb_2O_4 phases.

A biphasic, bulk mixed metal oxide system that has received quite a bit of attention with regard to oxygen transport is the bulk MoO_3–$Fe_2(MoO_4)_3$ catalyst system, which can further serve as a good model system for investigating the remote control hypothesis. According to the remote control model, the excess MoO_3 should play the role of an oxygen donor, which dissociates the gas phase molecular O_2 to atomic oxygen, that is then supplied to the acceptor $Fe_2(MoO_4)_3$ phase for methanol oxidation to formaldehyde. In situ Raman spectroscopic analysis of the bulk MoO_3/$Fe_2(MoO_4)_3$ catalyst during methanol oxidation demonstrated that the two catalytic phases are fully oxidized under reaction conditions, and thus, $Fe_2(MoO_4)_3$ would not benefit by the supply of additional oxygen from the crystalline MoO_3 phase if the remote control mechanism were operative.[130] Cyclic CH_3OH-TPSR studies with the $Fe_2(MoO_4)_3$ catalyst in the absence of gas phase molecular O_2 also revealed that this mixed oxide phase performs oxidation with oxygen being supplied from the bulk lattice, not gas phase, molecular O_2 (Mars–van Krevelen reaction mechanism).[28]

Recent in situ ultrarapid X-ray diffraction of $Fe_2(MoO_4)_3$ redox measurements have demonstrated that the reoxidation rate of iron molybdate with gaseous molecular O_2 is ~100 times faster than its reduction rate with gaseous H_2, which is consistent with the presence of a fully oxidized $Fe_2(MoO_4)_3$ phase under reaction conditions.[130] Furthermore, crystalline MoO_3 has been shown to only sluggishly supply bulk lattice oxygen to its surface and maintain the surface sites in their oxidized state.[59] This observation is further confirmed by elegant isotopic $H_2{}^{18}O$ Raman studies of the biphasic bulk MoO_3 and $Fe_2(MoO_4)_3$ system and found that although the bulk MoO_3 lattice remains unchanged, the bulk $Fe_2(MoO_4)_3$ lattice readily exchanges its lattice oxygen.[57]

Last, the presence of excess MoO_3 for the $Fe_2(MoO_4)_3$ phase does not increase the rate of methanol oxidation, as would be expected if the remote control mechanism were operating.[28]

dx.doi.org/10.1021/cs2005482 | ACS Catal. 2012, 2, 1235–1246

These fundamental studies, both individually and collectively, clearly demonstrate that there is no scientific basis for the remote control model of oxygen spillover from the donor phase to the acceptor phase during oxidation reactions over biphasic bulk mixed oxide phases.

IX. TURNOVER FREQUENCY (TOF) FOR BULK MIXED OXIDES

The turnover frequency and selectivity for methanol oxidation over one-component oxide catalysts are presented in Table 2 and indicate that compared with MoO_3, known for its outstanding redox properties, many of the one-component oxides are not dominated by redox properties (lower redox selectivity), but some oxides tend to exhibit quite high TOF_{redox} values.

The TOF and selectivity for methanol oxidation over the corresponding bulk mixed molybdates are presented in Table 3 and tend to exhibit much higher selectivity toward formaldehyde and much lower TOF values. An examination of the selectivity indicates that the selectivity toward formaldehyde markedly increased for most of bulk mixed molybdates relative to the corresponding one-component oxides. A closer examination of the TOF values of the bulk mixed molybdates reveals that they are more similar to that of pure MoO_3 rather than the one-component oxides. For example, the high TOF values for CoO, CuO, ZnO, and Bi_2O_3 are reduced by factors of 15−25 for the corresponding bulk mixed oxides, and the resultant TOF values are similar to those of crystalline MoO_3. The increase in selectivity toward formaldehyde is not surprising, since redox Mo cations are present on the surfaces of the bulk mixed molybdates, and redox Mo cations are not present on the surfaces of the one-component oxides, with the obvious exception of MoO_3.

Methanol-IR spectroscopy measurements reveal that Mo cations are the primary methanol chemisorption sites for mixed molybdates.[48] In addition, the TOF values for the bulk mixed molybdates are generally similar to that for the corresponding supported molybdenum oxide catalysts exclusively consisting of surface MoO_x species.[47] Similar findings were also reported for bulk vanadates, pure V_2O_5, and supported vanadium oxide catalysts.[131] The above findings strongly suggest that the catalytic properties of bulk mixed oxides are determined by the specific chemistry of the surface catalytic active sites (e.g., Mo or V cations). Clearly, there is also an influence of the metal ligand (Co, Ni, Cu, etc.) on the catalytic behavior of the cation (e.g., Mo or V), but this appears only to be a secondary effect. Therefore, the catalytic properties of bulk mixed oxides can be roughly estimated from their elemental outermost surface composition and characteristics of their individual surface cations.

X. NUMBER OF CATALYTIC ACTIVE SITES PARTICIPATING IN OXIDATION REACTIONS

Although many proposals have been made in the literature about the number of catalytic active sites participating in reactions by bulk mixed metal oxides (e.g., isolated sites,[14] multiple sites,[78] bifunctional sites[132−135]), there have not been any supporting data to back up these conjectures, since no surface composition and structural information was provided. It is, indeed, difficult to quantitatively control the nature of the surface catalytic active sites for bulk mixed oxides, since the surface compositions are generally not known and tend to be different from the bulk composition.[26]

Supported metal oxide catalysts, however, allow for quantitative control of the number and nature (redox, acidic or basic) of the surface catalytic active sites during the catalyst synthesis stage. Thus, supported metal oxide catalysts are model mixed oxide catalyst systems for determining the number of participating catalytic active sites for a targeted reaction.[136] With model supported metal oxide catalysts, it is straightforward to determine the number of metal oxide catalytic active sites involved in a specific reaction from the slope of log−log plot of catalytic activity (mol/g×h) vs MO_x loading (atoms/g). For two-electron redox reactions involving the consumption of one oxygen atom ($CH_3OH \rightarrow HCHO$,[137] $SO_2 \rightarrow SO_3$,[138] $H_2CH_2CH_3 \rightarrow H_2C{=}CHCH_3$,[139,140] $H_3CCH_3 \rightarrow H_2C{=}CH_2$,[141]) the slopes have been found to have a value of ∼1, indicating that only one catalytic active site is involved in these oxidation reactions. For four-electron redox reactions involving the consumption of two oxygen atoms ($H_2C{=}CHCH_3 \rightarrow H_2C{=}CHCHO$), the slope was found to have a value of ∼2, indicating that two catalytic active sites are involved in this oxidation reaction (one for removal of the two hydrogen atoms to form H_2O and a second for insertion of oxygen into the C_3 surface intermediate).[142] For more complex eight-electron redox reactions involving the consumption of four oxygen atoms (n-$C_4H_{10} \rightarrow$ cyclic $C_4H_2O_3$), multiple catalytic active sites involving bifunctional redox and acid sites are required.[143]

XI. NATURE OF OXYGEN SPECIES AND THEIR PARTICIPATION IN REDOX CATALYSIS

Bulk mixed oxides possess several different oxygen sites in their crystallographic bulk structure (e.g., M═O−M, M−O−M and OM_3)[144] as well as capping surface hydroxyls (e.g., M−OH, M_2−OH, and M_3OH) and surface oxygen functionalities (e.g., M═O).[145] Most of the bulk mixed oxide catalysts employed in selective oxidation reaction operate via the Mars−van Krevelen mechanism that involves the participation of bulk and surface lattice oxygen (O^{2-}), and the role of gas phase molecular O_2 is primarily to replenish the consumed oxygen from the catalyst bulk and surface lattice.[9] This is nicely demonstrated with temperature programmed surface reaction (TPSR) spectroscopy experiments (presented in Figure 4) that show that the oxidation reaction kinetics is identical when the experiments are conducted with and without gas phase molecular O_2.[28,29] During the Mars−van Krevelen reaction process, the reactant consumes oxygen from the redox catalytic active site (surface lattice), and this oxygen is initially replenished by diffusion of O^{2-} from the bulk lattice to the surface lattice. The diffusion of $^{16}O^{2-}$ anions from the bulk lattice to the surface lattice is directly observed (1) in the absence of gas phase molecular oxygen and (2) when gas phase isotopic $^{18}O_2$ is introduced as the oxidant during oxidation reactions and both the surface metal oxide catalytic active site and reaction products continue to contain ^{16}O.[122] Gas phase O_2 can also be present as physisorbed O_2* and chemisorbed O_2^-*, O_2^{2-}*, O^-* and O^{2-}* species on the surface of mixed metal oxides (the notation * is used to indicate that the oxygen species are coordinated to the oxide surfaces). The physisorbed O_2* and chemisorbed O_2^-*, and O_2^{2-}* molecular oxygen species form on nondefective, one-electron defect and two-electron defect sites on the oxide surface, respectively. Although these surface molecular oxygen

dx.doi.org/10.1021/cs2005482 | ACS Catal. 2012, 2, 1235−1246

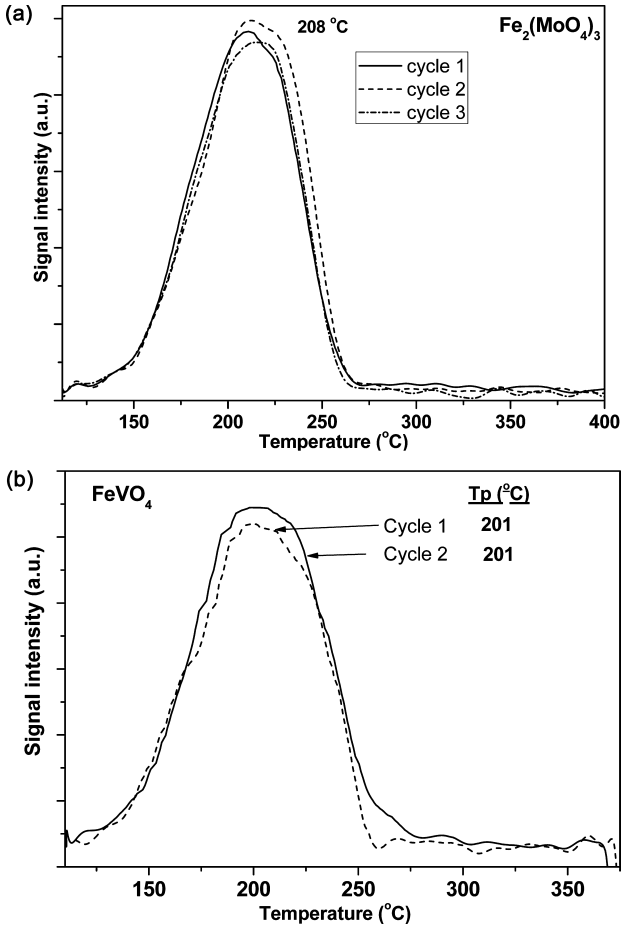

Figure 4. Cyclic $HCHO/CH_3OH$-TPSR spectra from the (a) bulk $Fe_2(MoO_4)_3$ and (b) bulk $FeVO_4$ catalysts (the catalysts were not reoxidized between the TPSR experiments).

species have been routinely invoked in the catalysis literature for many decades as catalytic active oxygen species, these species are not thermally stable at elevated temperatures and either desorb into the gas phase or readily decompose at subambient temperatures to form surface O^-* and O^{2-}* atomic species.[146] The atomic surface oxygen species may sometimes also participate in oxidation reactions (e.g., surface O^-* and O^{2-}* species appear to assist in H abstraction during dissociative chemisorption of propylene on the surfaces of mixed oxides).[147]

XII. DIFFUSION OF LATTICE OXYGEN

Information about oxygen diffusion through oxides can be obtained with isotope-exchange depth profiling (IEDP) after exposing an oxide to gaseous $^{18}O_2$ and subsequently analyzing the exchanged oxide while sputtering during secondary ion mass spectrometry (SIMS) and LEIS surface measurements.[148] SIMS (sampling depth of ~0.5−2.0 nm) and LEIS (sampling depth of ~0.3 nm) are excellent probes, since they can distinguish between the ^{18}O and ^{16}O isotopes. Such measurements can provide experimental information about the kinetics of ^{18}O diffusion through the oxide lattice and also surface oxygen exchange on oxides. Several such studies have been reported for yittria-stabilized zirconia (YSZ), $La_{1-x}Sr_xMnO_3$, and $Sm_{0.5}Sr_{0.5}CoO_3$ high temperature solid oxide fuel cells (SOFCs) after exposure to different conditions (with and without an applied bias). It was found from these studies that the ^{18}O exchange profile of a V-containing mixed oxide is dramatically altered under an electrical load because of the reduction of the vanadium oxidation state and the creation of oxygen vacancies. Furthermore, the presence of specific surface Ca impurities on YSZ can dramatically reduce the ^{18}O exchange process by reducing the number of surface sites available for oxygen exchange. Such new studies are beginning to provide quantitative kinetic information about exchange of gaseous molecular O_2 with mixed oxide surfaces and the diffusion of oxygen through the mixed oxide lattice.

CONCLUSIONS

A significant paradigm shift is taking place in catalysis by bulk mixed oxides. Over the past five decades, the focus has been to correlate the redox catalytic performance of bulk mixed oxide catalysts with their bulk crystalline structure. More recent studies, however, are recognizing that the catalytic process is a surface phenomenon and, consequently, the catalytic performance needs to be related to the outermost surface composition and structure. In the new model of bulk mixed oxide catalysts, the function of the bulk mixed oxide phase is to serve as a unique support for the surface catalytic active sites and as a source of bulk lattice oxygen. Fortunately, characterization techniques have become available to determine the composition of the outermost surface of bulk mixed oxides (LEIS, ER-XPS, and CH_3OH-IR), and further improvements in new methods for determining fundamental insights about the outermost surface layer are expected in the coming years. There are currently, however, no characterization methods that can provide the surface structure of bulk mixed oxides in powder form. Any developments in the determination of the surface structure of bulk mixed oxides would be extremely welcome and make a critical advance in the field of heterogeneous catalysis by bulk mixed oxides.

Some of the hypotheses and concepts in the bulk mixed metal oxide catalysis literature were quantitatively and systematically examined with one-component metal oxides, bulk mixed oxides, and model supported metal oxide catalysts. The findings sound a note of caution for the accepted hypotheses and concepts for catalysis by bulk mixed oxides, and new catalysis models need to be developed that are based on actual surface features of the bulk mixed oxide catalysts.

AUTHOR INFORMATION

Corresponding Author

*E-mail: iew0@lehigh.edu.

Notes

The authors declare no competing financial interest.

ACKNOWLEDGMENTS

The financial support provided by the U.S. Department of Energy-Basic Energy Sciences (Grant DE-FG02-93ER14350) and National Science Foundation (Grant 0609018) during the writing of this article is gratefully acknowledged.

REFERENCES

(1) Brazdil, J. F. In *Characterization of Catalytic Materials*; Wachs, I. E., Ed.; Butterworth-Heinemann: Boston, 1992, pp 47−66.

(2) Farrauto, R. J.; Bartholomew, C. H. *Fundamentals of Industrial Catalytic Processes*; John Wiley and Sons: Chichester, UK, 2003.

(3) Centi, G.; Cavani, F. *Selective Oxidation by Heterogeneous Catalysis*; Kluwer Publication: New York, 2001.

(4) Hodnett, B. K. *Heterogeneous Catalytic Oxidation: Fundamental and Technological Aspects of the Selective and Total Oxidation of Organic Compounds*; John Wiley & Sons: New York, 2000.
(5) Brundle, C. R.; Evans, C. A.; Wilson, S. *Encyclopedia of Materials Characterization*; Butterworth-Heinemann: Greenwich, CT, 1992.
(6) Boudart, M. In *Interactions on Metal Surfaces*, Gomer, R., Ed.; Springer-Verlag: Berlin, 1975, p 25.
(7) Somorjai, G. A. *Introduction to Surface Chemistry and Catalysis*; Wiley-Interscience: New York, 1994; p 271.
(8) Thomas, J. M.; Thomas, W. J. *Principles and Practice of Heterogeneous Catalysis*; VCH: New York, 1997, p 159.
(9) Mars, P.; van Krevelen, D. W. *Chem. Eng. Sci. (Spec. Suppl.)* **1954**, *3*, 41−57.
(10) Trifiro, F.; Centola, P.; Pasquon, I. *J. Catal.* **1968**, *10*, 86−88.
(11) Trifiro, F.; Pasquon, I. *J. Catal.* **1968**, *12*, 412−416.
(12) Tarama, K.; Teranishi, S.; Yoshida, S.; Tamura, N. *Proc. 3rd Int. Congr. Catal.*; Amsterdam, 1965, p 282.
(13) Haber, J.; Grzybowska, B. *J. Catal.* **1973**, *28*, 489−492.
(14) Grasselli, R. K. *Top. Catal.* **2001**, *15*, 93−101.
(15) Delmon, B. *Proc. 3rd Int. Conf. Chem. Uses Molybdenum*; Barry, H. F., Mitchell P. C. H., Eds.; Louvain-la-Neuve, Belgium, MI, 1979, p. 73
(16) Ozkan, U. S.; Schrader, G. L. *J. Catal.* **1985**, *95*, 120−136.
(17) Ozkan, U. S.; Schrader, G. L. *Appl. Catal., A* **1986**, *23*, 327−338.
(18) Ozkan, U. S.; Gill, R. C.; Smith, M. R. *J. Catal.* **1989**, *116*, 171−183.
(19) Delmon, B.; Ruiz, P. *React. Kinet. Catal. Lett.* **1987**, *35*, 303−314.
(20) Callahan, J. L.; Grasselli, R. K. *AIChE J.* **1963**, *9*, 755−760.
(21) Callahan, J. L.; Grasselli, R. K.; Milberger, E. C.; Strecker, H. A. *I&EC Prod. Res. Dev.* **1970**, *9*, 134−142.
(22) Grasselli, R. K.; Suresh, D. D.; Knox, K. *J. Catal.* **1970**, *18*, 356−358.
(23) Grasselli, R. K.; Suresh, D. D. *J. Catal.* **1972**, *25*, 273−291.
(24) Callahan, J. L.; Grasselli, R. K.; Knipple, W. R. US Patent 3 338 952, 1967.
(25) ter Veen, H. R. J.; Kim, T.; Wachs, I. E.; Brongersma, H. H. *Catal. Today* **2009**, *140*, 197−201.
(26) Merzlikin, S. V.; Tolkachev, N. N.; Strunskus, T.; Witte, G.; Glogowski, T.; Wöll, C.; Grünert, W. *Surf. Sci.* **2008**, *602*, 755−767.
(27) Merzlikin, S. V.; Tolkachev, N. N.; Briand, L. E.; Strunskus, T.; Woll, C.; Wachs, I. E.; Grunert, W. *Angew. Chem., Int. Ed.* **2010**, *49*, 8037−8041.
(28) Routray, K.; Zhou, W.; Kiely, C. J.; Gruenert, W.; Wachs, I. E. *J. Catal.* **2010**, *275*, 84−98.
(29) Routray, K.; Zhou, W.; Kiely, C. J.; Wachs, I. E. *ACS Catal.* **2011**, *1*, 54−66.
(30) Guliants, V. V.; Benziger, J. B.; Sundaresan, S.; Yao, N.; Wachs, I. E. *Catal. Lett.* **1995**, *32*, 379−386.
(31) Sanfiz, A. C.; Hansen, T. W.; Girgsdies, F.; Timpe, O.; Rodel, E.; Ressler, T.; Trunschke, A.; Schlogl, R. *Top. Catal.* **2008**, *50*, 19−32.
(32) Shvets, V. A.; Sarichev, M. E.; Kazansky, V. B. *J. Catal.* **1968**, *11*, 378−379.
(33) Parekh, B. S.; Weller, S. W. *J. Catal.* **1977**, *47*, 100−108.
(34) Ramanathan, K.; Weller, S. W. *J. Catal.* **1985**, *95*, 249−259.
(35) Nag, N. K.; Chary, K. V. R.; Reddy, B. M.; Rama Rao, B.; Subrahmanyam, V. S. *Appl. Catal.* **1984**, *9*, 225−233.
(36) Reddy, B. M.; Chary, K. V. R.; Rama Rao, B.; Subrahmanyam, V. S.; Sunandana, C. S.; Nag, N. K. *Polyhedron* **1986**, *5*, 191−194.
(37) Nag, N.; Chary, K.; Subrahmanyam, V. *J. Chem. Soc., Chem.Commun.* **1986**, 1147−1148.
(38) Chary, K. V. R. *J. Chem. Soc., Chem. Commun.* **1989**, *2*, 104−105.
(39) Chary, K. V. R.; Vijayakumar, V.; Rao, P. K. *Langmuir* **1990**, *6*, 1549−1550.
(40) Chary, K. V. R.; Rama Rao, B.; Subrahmanyam, V. S. *Appl. Catal.* **1991**, *74*, 1−13.
(41) Desikan, A. N.; Huang, L.; Oyama, S. T. *J. Phys. Chem.* **1991**, *95*, 10050−10056.
(42) Majunke, F.; Baerns, M.; Baiker, A.; Koeppel, R. A. *Catal. Today* **1994**, *20*, 53−59.
(43) Reddy, B. M.; Manohar, B.; Reddy, E. P. *Langmuir* **1993**, *9*, 1781−1785.
(44) Arena, F.; Frusteri, F.; Parmaliana, A. *Appl. Catal., A* **1999**, *176*, 189−199.
(45) Tatibouët, J. M. *Appl. Catal., A* **1997**, *148*, 213−252.
(46) Briand, L. E.; Farneth, W. E.; Wachs, I. E. *Catal. Today* **2000**, *62*, 219−229.
(47) Briand, L. E.; Hirt, A. M.; Wachs, I. E. *J. Catal.* **2001**, *202*, 268−278.
(48) Burcham, L. J.; Briand, L. E.; Wachs, I. E. *Langmuir* **2001**, *17*, 6175−6184.
(49) Burcham, L. J.; Badlani, M.; Wachs, I. E. *J. Catal.* **2001**, *203*, 104−121.
(50) Park, J.-W.; Potvin, C.; Djega-Mariadassou, G. *Top. Catal.* **2007**, *42*, 259−262.
(51) Guliants, V. V.; Bhandari, R.; Hughett, A. R.; Bhatt, S.; Schuler, B. D.; Brongersma, H. H.; Knoester, A.; Gaffney, A. M.; Han, S. *J. Phys. Chem. B* **2006**, *110*, 6129−6140.
(52) Burcham, L. J.; Briand, L. E.; Wachs, I. E. *Langmuir* **2001**, *17*, 6164−6174.
(53) Farneth, W. E.; Ohuchi, F.; Staley, R. H.; Chowdhry, U.; Sleight, A. W. *J. Phys. Chem.* **1985**, *89*, 2493−2497.
(54) Farneth, W. E.; Staley, R. H.; Sleight, A. W. *J. Am. Chem. Soc.* **1986**, *108*, 2327−2332.
(55) Machiels, C. J.; Chowdhry, U.; Harrison, W. T. A.; Sleight, A. W. *ACS Symp. Ser.* **1985**, *279*, 103−119.
(56) Machiels, C. J.; Sleight, A. W. In Proc. of the 4th Int. Confer., Chem. Uses Molybdenum; Ann Arbor, MI, 1982; Barry, H. F., Mitchell, P. C. H., Eds.; Climax Molybdenum Co.: MI, 1982, p 411.
(57) Machiels, C. J.; Chowdhry, U.; Sleight, A. W. 186th Natl. Meeting Am. Chem. Soc., Div. Petrol. Chem., Washington, DC, 28 August−2 September, 1983, American Chemical Society: Washington, DC, 1983, p 1293.
(58) Chowdhry, U.; Ferretti, A.; Firment, L. E.; Machiels, C. J.; Ohuchi, F.; Sleight, A. W.; Staley, R. H. *Appl. Surf. Sci.* **1984**, *19*, 360−372.
(59) Wachs, I. E.; Jehng, J.-M.; Ueda, W. *J. Phys. Chem. B* **2005**, *109*, 2275−2284.
(60) Boudart, M. *Kinetics of Chemical Processes*; Princeton University Press: Princeton, NJ, 1984.
(61) Bond, G. C.; Flamerz, S.; Wiik, L. V. *Catal. Today* **1987**, *1*, 229−243.
(62) Desikan, A. N.; Huang, L.; Oyama, S. T. *J. Phys. Chem.* **1991**, *95*, 10050−10056.
(63) Chary, K. V. R.; Vijayakumar, V.; Rao, P. K. *Langmuir* **1990**, *6*, 1549−1550.
(64) Sleight, A.; Staley, R.; Chowdhury, U.; Badlani, M.; Wachs, I. E. *Catal. Lett.* **2001**, *75*, 137−149.
(65) Routray, K.; Briand, L. E.; Wachs, I. E. *J. Catal.* **2008**, *256*, 145−153.
(66) Fein, D. E.; Wachs, I. E. *J. Catal.* **2002**, *210*, 241−254.
(67) Kulkarni, D.; Wachs, I. E. *Appl. Catal., A* **2002**, *237*, 121−137.
(68) Guliants, V. V.; Bhandari, R.; Brongersma, H. H.; Knoester, A.; Gaffney, A. M.; Han, S. *J. Phys. Chem. B* **2005**, *109*, 10234−10242.
(69) Guliants, V. V.; Brongersma, H. H.; Knoester, A.; Gaffney, A. M.; Han, S. *Top. Catal.* **2006**, *38*, 41−50.
(70) Badlani, M.; Wachs, I. E. *Catal. Lett.* **2001**, *75*, 137−149.
(71) Chowdhry, U.; Ferretti, A.; Firment, L. E.; Machiels, C. J.; Ohuchi, F.; Sleight, A. W.; Staley, R. H. *Appl. Surf. Sci.* **1984**, *19*, 360−372.
(72) Boreskov, G. In *Catalysis Science and Technology*; Anderson, J. R., Boudart, M., Eds.; Springer: New York, 1982; Vol. 3, p 62.
(73) Machiels, C. J.; Sleight, A. W. *J. Catal.* **1982**, *76*, 238−239.
(74) Ross-Medgaarden, E. I.; Knowles, W. V.; Kim, T.; Wong, M. S.; Zhou, W.; Kiely, C. J.; Wachs, I. E. *J. Catal.* **2008**, *256*, 108−125.
(75) Sachtler, W. M. H.; De Boer, N. H. *Proc. 3rd Int. Congr. Catal.*, Amsterdam, 1964 Wiley: New York, 1965, p 240.

(76) Sachtler, W. M. H.; Dorgelo, G. J. H.; Fahrenfort, J.; Voorhoeve, R. J. H. In *Proc. 4th Int. Congr. Catal.*, Moscow, 1968 Kazanskv, B. A., Ed.; Adler: New York, 1968; p 454.
(77) Bordes, E. *Catal. Today* **1987**, *1*, 499−526.
(78) Centi, G.; Trifiro, F.; Ebner, J. R.; Franchetti, V. M. *Chem. Rev.* **1988**, *88*, 55−80.
(79) Horowitz, H. S.; Blackstone, C. M.; Sleight, A. W.; Teufer, G. *Appl. Catal.* **1988**, *38*, 193−210.
(80) Harrouch Batis, N.; Batis, H.; Ghorbel, A.; Vedrine, J. C.; Volta, J. C. *J. Catal.* **1991**, *128*, 248−263.
(81) Hutchings, G. *Appl. Catal.* **1991**, *72*, 1−32.
(82) Centi, G. *Catal. Today* **1993**, *16*, 5−26.
(83) Agaskar, P. A.; DeCaul, L.; Grasselli, R. K. *Catal. Lett.* **1994**, *23*, 339−351.
(84) Shelef, M.; Wheeler, M. A. Z.; Yao, H. C. *Surf. Sci.* **1975**, *47*, 697−703.
(85) Yao, H. C.; Shelef, M. *J. Phys. Chem.* **1974**, *78*, 2490−2496.
(86) Jacobs, J. P.; Maltha, A; Reintjes, J. G. H.; Drimal, J.; Ponec, V.; Brongersma, H. H. *J. Catal.* **1994**, *147*, 294−300.
(87) Strohmeier, B. R.; Hercules, D. M. *J. Catal.* **1984**, *86*, 266−279.
(88) Brongersma, H. H.; Jacobs, J.-P. *Appl. Surf. Sci.* **1994**, *75*, 133−138.
(89) Mulcahy, F. M.; Houalla, M.; Hercules, D. M. *Anal. Chem.* **1990**, *62*, 2232−2236.
(90) Drawdy, J. E.; Hoflund, G. B.; Gardner, S. D.; Yngvadottir, E. A.; Schryder, D. R. *Surf. Interface Anal.* **1990**, *16*, 369−374.
(91) Prada Silvy, R.; Beuken, J. M.; Fierro, J. L. G.; Bertrand, P.; Delmon, B. *Surf. Interface Anal.* **1986**, *8*, 167−172.
(92) Kasztelan, S.; Grimblot, J.; Bonnelle, J. P. *J. Phys. Chem.* **1987**, *91*, 1503−1508.
(93) Taugler, E.; Knozinger, H. In *Surface Science, Principles and Applications*; Howe, R. F., Lamb, R. N., Wandlet, K., Eds.; Springer-Verlog: Berlin, 1993; pp 264.
(94) Brongersma, H. H.; Groenen, P. A. C.; Jacobs, J. P. In *Science of Ceramic Interfaces II*; Nowotny, J., Ed.; Elsevier Science B.V.: Amsterdam, 1994; pp 113−182.
(95) Fullarton, I. C.; Jacobs, J.-P.; van Benthem, H. E.; Kilner, J. A.; Brongersma, H. H.; Scanlon, P.; Steele, B. C. H. *Ionics* **1995**, *1*, 51−58.
(96) Rosnik, J.; Jacobs, J.-P.; Brongersma, H. H. In *Surfaces, Vacuum, and their Applications*; Hernández-Calderón, I., Asomoza, R., Eds.; AIP Press: Woodbury, NY, 1996; Vol. *378*; pp 44−51.
(97) Viitanen, M. M.; von Welzenis, R. G.; Brongersma, H. H.; van Berkel, F. P. F. *Solid State Ionics* **2002**, *150*, 223−228.
(98) Yao, H. C.; Yu Yao, Y. F. *J. Catal.* **1984**, *86*, 254−265.
(99) Fornasiero, P.; Balducci, G.; Kaspar, J.; Meriani, S.; Monte, R.; Graziani, M. *Catal. Today* **1996**, *29*, 47−52.
(100) Murota, T.; Hasegawa, T.; Aozasa, S.; Matsui, H.; Motoyama, M. *J. Alloys Compd.* **1993**, *193*, 298−299.
(101) Cho, B. K. *J. Catal.* **1991**, *131*, 74−87.
(102) Balducci, G.; Fornasiero, P.; Monte, R.; Kaspar, J.; Meriani, S.; Graziani, M. *Catal. Lett.* **1995**, *33*, 193−200.
(103) Fornasiero, P.; Balducci, G.; Monte, R.; Kaspar, J.; Sergo, V.; Gubitosa, G.; Ferrero, A.; Graziani, M. *J. Catal.* **1996**, *164*, 173−183.
(104) Vlaic, G.; Monte, R.; Fornasiero, P.; Fonda, E.; Kaspar, J.; Graziani, M. *J. Catal.* **1999**, *182*, 378−389.
(105) Hori, C. E.; Permana, H.; Ng, K. Y. S.; Brenner, A.; More, K.; Rahmoeller, K. M.; Belton, D. *Appl. Catal., B* **1998**, *16*, 105−117.
(106) Finocchio, E.; Daturi, M.; Binet, C.; Lavalley, J. C.; Blanchard, G. *Catal. Today* **1999**, *52*, 53−63.
(107) Jansen, W. P. A.; Ruitenbeek, M.; v.d. Gon, A. W. D.; Geus, J. W.; Brongersma, H. H. *J. Catal.* **2000**, *196*, 379−387.
(108) Guliants, V. V.; Bhandari, R.; Brongersma, H. H.; Knoester, A.; Gaffney, A. M.; Han, S. *J. Phys. Chem. B* **2005**, *109*, 10234−10242.
(109) Busca, G. *J. Mol. Catal.* **1989**, *50*, 241−249.
(110) Jehng, J.-M.; Wachs, I. E. *Chem. Mater.* **1991**, *3*, 100−107.
(111) Busca, G. *J. Catal.* **1989**, *120*, 303−313.
(112) Holstein, W. L.; Machiels, C. J. *J. Catal.* **1996**, *162*, 118−124.
(113) Burcham, L. J.; Wachs, I. E. *Catal. Today* **1999**, *49*, 467−484.
(114) Hardcastle, F. D.; Wachs, I. E. *J. Raman Spectrosc.* **1990**, *21*, 683−691.
(115) Hardcastle, F. D.; Wachs, I. E. *J. Phys. Chem.* **1991**, *95*, 5031−5041.
(116) Morooka, Y.; Ozaki, A. *J. Catal.* **1966**, *5*, 116−124.
(117) Moro-Oka, Y.; Morikawa, Y.; Ozaki, A. *J. Catal.* **1967**, *7*, 23−32.
(118) Sachtler, W. M. H.; de Boer, N. H. *3rd Int. Congr. Catal.* **1964**, I−6.
(119) Soares, A. P. V.; Portela, M. F.; Kiennemann, A. *Catal. Rev. Sci. Eng.* **2005**, *47*, 125−174.
(120) Okamoto, Y.; Morikawa, F.; Oh-Hiraki, K.; Imanaka, T.; Teranishi, S. *J. Chem. Soc. Chem. Commun.* **1981**, 1018−1019.
(121) Cadus, L. E.; Xiong, Y. L.; Gotor, F. J.; Acosta, D.; Naud, J.; Ruiz, P.; Delmon, B. *Stud. Surf. Sci. Catal.* **1994**, *82*, 41−54.
(122) Soderhjelm, E.; House, M. P.; Cruise, N.; Holmberg, J.; Bowker, M.; Bovin, J.-O.; Andersson, A. *Top. Catal.* **2008**, *50*, 145−155.
(123) Martin, D.; Kaur, P.; Duprez, D.; Gaigneaux, E.; Ruiz, P.; Delmon, B. *Catal. Today* **1996**, *32*, 329−336.
(124) Ruiz, P.; Delmon, B. *Catal. Today* **1988**, *3*, 199−209.
(125) Knozinger, H. *Catal. Today* **1996**, *32*, 71−80.
(126) Wang, C. B.; Cai, Y.; Wachs, I. E. *Langmuir* **1999**, *15*, 1223−1235.
(127) Haber, J. *Pure Appl. Chem.* **1984**, *56*, 1663−1676.
(128) Xie, Y. C.; Tang, Y. Q. *Adv. Catal.* **1990**, *37*, 1−43.
(129) Knozinger, H.; Taglauer, E. *Catalysis* **1993**, *10*, 1−40.
(130) Wilson, J. A.; Hill, C. G.; Dumesic, J. A. *J. Mol. Catal.* **1990**, *61*, 333−352.
(131) Briand, L. E.; Jehng, J.-M.; Cornaglia, L.; Hirt, A. M.; Wachs, I. E. *Catal. Today* **2003**, *78*, 257−268.
(132) Matsuura, I.; Schuit, G. C. A. *J. Catal.* **1972**, *25*, 314−325.
(133) Haber, J.; Grzybowska, B. *J. Catal.* **1973**, *28*, 489−492.
(134) Linn, W. J.; Sleight, A. W. *Ann. N.Y. Acad. Sci.* **1976**, *272*, 22−44.
(135) Burrington, J. D.; Kartisek, C. T.; Grasselli, R. K. *J. Catal.* **1980**, *63*, 235−254.
(136) Wachs, I. E. *Catal. Today* **2005**, *100*, 79−94.
(137) Kim, T.; Wachs, I. E. *J. Catal.* **2008**, *255*, 197−205.
(138) Dunn, J. P.; Stenger, H. G., Jr.; Wachs, I. E. *J. Catal.* **1999**, *181*, 233−243.
(139) Zhao, Z.; Gao, X.; Wachs, I. E. *J. Phys. Chem. B* **2003**, *107*, 6333−6342.
(140) Gao, X.; Jehng, J.-M.; Wachs, I. E. *J. Catal.* **2002**, *209*, 43−50.
(141) Martínez-Huerta, M. V.; Gao, X.; Tian, H.; Wachs, I. E.; Fierro, J. L. G.; Banares, M. A. *Catal. Today* **2006**, *118*, 279−287.
(142) Zhao, C.; Wachs, I. E. *J. Catal.* **2008**, *257*, 181−189.
(143) Wachs, I. E.; Jehng, J.-M.; Deo, G.; Weckhuysen, B. M.; Guliants, V. V.; Benziger, J. B.; Sundaresan, S. *J. Catal.* **1997**, *170*, 75−88.
(144) Wells, A. F. *Structural Inorganic Chemistry*; Oxford University Press: New York, 1984.
(145) Davydov, A. *Molecular Spectroscopy of Oxide Catalyst Surfaces*; John Wiley and Sons: West Sussex, England, 2003.
(146) Wachs, I. E.; Roberts, C. A. *Chem. Soc. Rev.* **2010**, *39*, 5002−5017.
(147) Zhao, C.; Wachs, I. E. *J. Phys. Chem. C* **2008**, *112*, 11363−11372.
(148) Kilner, J. A.; Skinner, S. J.; Brongersma, H. H. *J. Solid State Electrochem.* **2011**, *15*, 861−876.